Anbar Journal of Engineering Science (AJES) **Vol. 17 , No. 1 (2026) , pp. 45 ~ 58**
P-ISSN: 1997-9428; E-ISSN: 2706-7440 **DOI: http://doi.org/10.37649/AJES.25.0043**

University of Anbar

Anbar Journal of Engineering Science

journal homepage: https://ajes.uoanbar.edu.iq/

Optimal Economic Operation of CCHP Micro grids with High Renewable Energy Integration

Mohammed Salam Abdulghafoor [a], Mohammed K. Al-Saadi [b], Ameer Abed Jaddoa [c]
[a b c] *Electromechanical Engineering Department, University of Technology, Baghdad, Iraq*
Email: eme.23.06@grad.uotechnology.edu.iq ; ORCID: https://orcid.org/0009-0004-0851-8645
Email: 50055@uotechnology.edu.iq ; ORCID: https://orcid.org/0000-0001-6424-4328
Email: Ameer.A.Jaddoa@uotechnology.edu.iq ; ORCID: https://orcid.org/0000-0001-5158-1827

PAPER INFO

Received: 09 /12/2025
Revised: 15 /03/2026
Accepted: 25/04/2026

Keywords:
CCHP
Unit commitment
Optimization programs
scheduling
multi-objective energy

ABSTRACT

CCHP (combined cooling, heating, and power) systems make substantial use of renewable energy. Establishing a versatile, low-carbon, multi-energy complementary energy system is crucial. However, the performance of the system can be impacted in a variety of ways by mixing different renewable energy sources system. This study suggests an ideal planning strategy to reduce the distribution grid-based CCHP's overall operational and environmental costs. The proposed optimization problem in this work is formulated as a mixed integer nonlinear program with interval (MINLP). In order to offer heat, cool and electricity at the lowest feasible operational and emission costs, the unit commitment (UC) method is made to respond to the energy and thermal energy production of the distribution system. The proposed system consists of multiple generation units integrated within a CCHP microgrid and is evaluated based on hourly load demand, renewable energy inputs, and electricity price profiles to reduce overall operating and emission costs. The results showed that when the system was connected to the network, the total cost decreased to 739 $ after it had been 1202.62 $ when disconnected.

1. Introduction

All electrical power generating systems that use recoverable waste heat for home hot water, space heating, and cooling are referred to as CCHP (combined cooling, heating, and power) systems [1]. Due to its higher overall performance, the CCHP system is preferred globally [2][3]. It can improve the power supply, lower resource consumption, enhance the environment, and encourage sustainable growth by combining new and renewable energy sources [4][5]. The primary concerns that prompt increased attention to the development of low emission multi energy systems are the depletion of fossil fuels, environmental contamination, and rising energy demand [6]

Recent studies have been a lot of study done recently on the CCHP system, which combines geothermal, wind, biomass, solar, and other renewable energy sources [7]. Building a microgrid inside the main network that positions energy sources close to the end user to meet their requirements is one of the innovative solutions to this problem, which calls for a control technology to allocate capacities and loads between these

* Corresponding author: Ameer Abed Jaddoa; ameer.A.Jaddoa@uotechnology.edu.iq ; +964-7736833726

systems [8][9][10][11][12][13]. A microgrid (MG) is an autonomously controlled low-voltage distribution network that may be used in both isolated (island) and grid-connected modes. MG uses a variety of power sources, including distributed generation (DG), microturbines (MTs), and renewable energy (RE). Technologies for energy storage are also in place to optimize resource use and ensure that the actual demand for response is satisfied [14]. When renewable energy sources are stochastic and demand is unpredictable, integrating them with the grid presents challenges. Furthermore, Furthermore, grid stability is adversely affected because peak renewable energy generation often occurs during periods of low demand [15]. MG may have a heat system in addition to the electrical system, which is called utilizing solar energy for heating applications away from electricity generation through the use of solar air heaters (SAH) or solar collectors, as well as combined heat and power microgrid CHP-MG to respond to heat sources' demand for heat, numerous optimization techniques, such as unit commitment (UC), heuristic algorithms, genetic algorithms (GA), particle swarm optimization (PSO), and others, were used to reduce costs and emissions while improving the reliability and stability of electricity networks ,in addition to using the waste heat released during the energy generating process for heating systems [16][17][18][19][20].

Ma et al. [21] proposed an interval scheduling technique for CCHP systems integrated with solar energy to enhance system performance. Using an electrical tracking approach, the annual total cost-saving rate (ATCSR) and the CCHP system are compared, Jia et al. [22] developed a novel CCHP system that integrates a solar thermal (ST) and an organic Rankine cycle. In study [23] Soheyli et al, proposed a CCHP system using solar (PV), wind turbines, and solid oxide fuel cells as the main motors. To determine the optimal amount of each system component, they used a multi-objective particle swarm optimization approach. Further investigation, Ren et al. [24] a hybrid CCHP system was optimized and compared for three buildings with varying operating circumstances. A photovoltaic thermal solar collector (PVT) in system A transforms solar energy into heat and electricity, whereas a photovoltaic solar collector (PVT) in system B transforms solar energy into thermal and electrical energy. Ge et al. [25] explored three different design scenarios and investigated the optimal method for setting up a solar-assisted natural gas-distributed energy system with energy storage. The findings indicate that the ATCs of the solar-assisted natural gas DES with energy storage (Scenario 3) and the solar-powered DES (Scenario 2) are decreased by 2.90% and 7.48%, respectively, as compared to the traditional DES (Scenario 1).

Stanek et al. [26] developed a sustainability evaluation for CCHP systems amidst uncertainty using ANP–AHP–TOPSIS methodologies. The results underscore the significance of including renewable sources and multi-criteria assessment in the design of CCHP systems., Ruan et al. [27] developed a deep reinforcement learning technique to optimize combined cooling, heating, and power systems including renewable energy and energy storage. The DRL controller independently regulates power, heating, and cooling flows to save expenses. .In study [28], Song et al, combined solar and geothermal energy, two renewable energy sources, with the power system to enable the generation of power using renewable energy. The results showed that the thermal efficiency of the linked power station was 11.21% higher than that of the independent air-cooled geothermal ORC power station. Previous studies can be classified into deterministic and stochastic models, as well as heuristic and mathematical optimization approaches.

In current study proposed an energy management strategy for microgrids that mainly integrates CCHP-MG with renewable sources to meet electrical, thermal, and cooling demands. A power MG, micro-electric system, micro-heat system, and micro-cool system build up the CCHP. In addition to renewable sources (WT) wind turbine, (SAH) solar air heater, and PV, these systems are connected to one another via MT, FC, gas boiler (GB), electric heater (EH), electric chiller (EC), absorption chiller (AC), and P2G technology. This was implemented in order to determine which design provides the lowest operational costs for the system. The system was also connected to the utility grid, enabling continuous interchange, as it purchases energy when it is unable to meet its output and sells energy when there is extra production based on demand response. The exchange power in MG was integrated using julia software and the Mixed-Integer Non-Linear Programming (MINLP) approach. The multi-target target function was modified to enhance the unilateral target by

considering the monetary concept of the costs of carbon dioxide (CO_2), sulfur dioxide (SO_2), nitrogen oxide (NO_x), and particulate matter (PM) during the 24-hour assessment of the network's electrical, heating, and cooling systems' operational registration. Despite the extensive research on CCHP systems, several limitations still exist, particularly in the integration of renewable energy sources and the simultaneous consideration of economic and environmental objectives. Most previous studies have focused on either cost optimization or system performance without adequately addressing emission reduction. Therefore, this study aims to develop an optimized energy management framework that enhances both economic efficiency and environmental performance. In contrast to existing studies, this work presents an integrated optimization strategy that improves both economic and environmental performance

2. Modeling the Proposed System's Components Mathematically

The study combines numerical optimization with experimental data obtained from the solar air heater (SAH) setup. The boundary conditions include measured thermal performance data along with predefined load and energy profiles. The mathematical model consists of several key components, including electrical balance, thermal balance, cooling system modeling, and cost optimization. The main equations governing these components are described below:

2.1 Subsystem of Electricity

2.1.1 Diesel Generator model

A diesel generator in this research, an internal combustion diesel fuel generatorwas used to provide electricity during peak hours. The following linear equation may be used to describe fuel consumption: C_{DG} is the cost of fuel consumption by utilizing DG in ($), η_DG is the efficiency of DG, and P_{DG}^{t} t is the output electrical power from FC at each time in (KWh), the U_{DG} are on/off state of DG [31].

$$C_{DG}{}^{t} = U_{DG}{}^{t}(a\, P_{DG}^{t}{}^{2} + b\, P_{DG}^{t} + c) \quad (1)$$

2.1.2 Microturbines model

MT-based CHP is examined as a simultaneous source of heat and electricity. NG is used to power microturbines. The following formula is used to calculate the amount of gas consumed [32].

$$C_{MT}^{t} = \frac{U_{MT}{}^{t} * P_{MT}^{t}}{LCV * \eta_{MT}} * \beta_g \quad (2)$$

LCV is minimum value of natural gas heating (KWh/m^3), βg is the price of natural gas ($\$/m^3$), P_{MT}^{t} is the electrical power output from MT at each time in KWh, and C_{MT} is the fuel consumption cost of the microturbine in ($), the U_{MT} are on/off state of MT.

H_{MT}^{t} in (KW) may be written as follows:

$$H_{MT}^{t} = \frac{P_{MT}^{t}\,(1-\eta_{MT}-\eta_l)\eta_{HR}}{\eta_{MT}} \quad (3)$$

Where η_l is the heat loss factor, η_{HR} is the heat recovery efficiency. The recovered heat is modeled as a function of the microturbine power output and its thermal efficiency, reflecting practical energy conversion behavior [32].

2.1.3 Fuel cell model

In this study, a proton membrane fuel cell (FC) was used to convert the chemical energy contained in the gas into electrical energy, which was then used as a source of power. The following linear equation may be used to depict fuel consumption: $C_{FC}$is the fuel consumption cost while utilizing a fuel cell in ($), η_FC is the efficiency of FC, and $P_{FC}^{t}$is the electrical power production from FC at each time in (KWh) [33]. the U_{FC} are on/off state of FC.

$$C_{FC}{}^{t} = \frac{U_{FC}^{t} * P_{FC}^{t}}{LCV * \eta_{FC}} * \beta_g \quad (4)$$

2.1.4 Battery model

The SB's operation is governed by the following formula. [31].

$$SOC_b^t = SOC_b^{t-1} - \frac{P_{b.dis}^{t}}{\eta_{b.dis}} + P_{b.ch}^{t}\ \eta_{b.ch} \quad (5)$$

where the SOC charge level at time t is represented at time t-1. The power that is delivered and absorbed is $P_{b.ch}^{t}$ *and* $P_{b.dis}^{t}$. The efficiencies are ηch and ηdis. Δt is the operating time interval. The

following formula is used to determine the SB operation's cost:

$$C_b^t = P_b^t * \omega_b \quad (6)$$

where C_b^t represents the SB's operating costs.

2.1.5 Power and utilty grid exchange

The cost is calculated as follows, and Energy exchange between the main system and the CCHP system is possible.

$$C_{e.UG}^t = P_{UG}^t * \omega_{elect.}^t \quad (7)$$

Where The power trading cost $C_{e.UG}^t$ in deponed on electrical price $\omega_{elect.}^t$ in ($\$/KWh$).

2.1.5 Emmission cost model

Emissions of carbon dioxide (CO_2), sulfur dioxide (SO_2), nitrogen oxides (NO_x), and particulate matter (PM) harm the ecosystem and contaminate the weather, the following formula is used to convert them to expenses:

$$C_{Emi.}^t = \sum_1^i \sum_1^j P_i^t \, C_j \, E_{i,j} \quad (8)$$

The power product that may affect the greenhouse gasses of i^{th}, in this study is P_i^t (KWh), which includes DG, MT, and FC. The cost of emission for the j^{th} GHG in this study is C_j in ($/Kg), which includes CO_2, SO_2, NO_x, and PM. The quantity of can emission j^{th}, where product power for each i^{th}, is represented by the $E_{i,j}$ in (Kg·KWh) [34]. The parameter of emmisions shown in table 2.

2.2 Subsystem of heating

2.2.1 Solar air heater model

In this research, solar energy was converted into useful thermal energy using a solar air heater (SAH). To see how they influenced performance, aluminum cans were put up. The experimental results are consistent with commonly reported. The measurements were obtained using standard instruments with acceptable accuracy and ambient temperature during the specified measurement period as shown in figure 1 [35].

The value of H_{SAH}^t was measured experimentally for this study, table (1), whereas T_o, T_i are the air outlet and inlet temperature averages C°, C_p is the air specific heat in KJ/Kg*K, and $\dot{m}^\circ$ is the mass flow rate in the SAH duct in kg/s.

The rate of heat transfer for SAH H_{SAH}^t in (KW) can be expressed by:

$$H_{SAH}^t = \dot{m}^\circ * C_p * (T_o - T_i) \quad (9)$$

Figure 1. Experimental setup of the solar air heater (SAH) in this research

2.2.2 Gas boiler model

Heat was generated in the Gas Boiler GB by using natural gas. The following is a statement of the cost of using natural gas in the gas boiler to generate heat C_{MT} in ($).as follows:

$$C_{GB}{}^t = \frac{H_{GB}^t}{LCV * \eta_{GB}} * p_g \quad (10)$$

In accordance with the maintenance cost rate coefficient $K_{om.MT}$ in ($/KWh), the maintenance cost of MT $C_{om.MT}$

$$C_{om.GB}^t = H_{GB}^t * K_{om.GB} \quad (11)$$

All parameters have been shown in table 5.

2.2.3 Heat storage battery model

The following formula represents the HS operation

$$SOC_{hs}^t = SOC_{hs}^{t-1}(1 - RH) - \frac{H_{hs.dis}^t}{\eta_{hs.dis}} + H_{hs.ch}^t \quad (12)$$

the charging and discharging power represent by $H_{hs.ch}^t$, $H_{hs.dis}^t$ and $\eta_{hs.ch}, \eta_{hs.dis}$ are the charging and discharging efficiency. RH is the heat loss rate [36].

2.2.4 Heat and utilty grid exchange

The following formula represents the cost of heat energy exchanges with the main grid:

$$C^t_{h.UG} = H^t_{UG} * \omega^t_{heat.} \quad (13)$$

where the heat power exchange with the main grid is represented by H^t_{UG}. Selling power requires a negative value, while purchasing power requires a positive value. The open market price of heat energy is represented by the $\omega^t_{heat.}$.

2.2.5 Electric heater model

The thermal loads receive heat from the EH, and the output heat, H^t_{EH} in (KW), is shown as follows:

$$H^t_{EH} = P^t_{EH} * \eta_{EH} \quad (14)$$

and EH $C_{om.EK}$ maintenance cost based on the $K_{om.EH}$ maintenance cost rate coefficient in ($/KWh) .

$$C^t_{om.EH} = H^t_{EH} * K_{om.EH} \quad (15)$$

2.3 Cooling subsystem

2.3.5 Electric chiller model

By using cooling power, the electric chiller satisfies the cooling need. The following formula represents the EC's output cooling power.:

$$\text{Cec(t)} = \text{Pec(t)} \,.\, COP_{ec} \quad (16)$$

When the electric power provided to EC is represented by Pec(t) and the coefficient of performance is represented by (COP_{ec}).

2.3.5 Absorber chiller model

The absorption chiller provides the cooling load with cooling power. The AC's output cooling power is calculated using the formula below:

$$\text{Cac(t)} = \text{Hac(t)} \,.\, COP_{ac} \quad (17)$$

where (COP_{ac}). is the coefficient of performance and Hac(t) is the heat that is given to AC. The parameters have been shown in table 5.

3. Energy balance constrains

a. The electrical balance equation ensures that the total power generated from all available sources is equal to the electrical demand at each time step, thereby maintaining system stability.

$$P^t_{MT} + P^t_{FC} + P^t_{DG} + P^t_{RE} + P^t_{b.dis} + P^t_{import} = P^t_{export} + P^t_{b.ch} + P^t_{ce} + P^t_{EH} + L^t_{elctr} \quad (18)$$

Where $L^t_{elctr.}$ It is a load that requires electrical power in (KWh) and P^t_{RE} represents power of renewable energy such as wind and pv.

b. The thermal balance equation guarantees that the total heat produced from various units meets the required thermal demand and storage conditions within the system and exported energy at each time step.

$$H^t_{MT} + H^t_{GB} + P^t_{SAH} + H^t_{EH} + H^t_{b.dis} + H^t_{import} = H^t_{export} + H^t_{b.ch} + H^t_{ca} + L^t_{heat} \quad (19)$$

Where $L^t_{heat.}$ it is heat power demand load in (KWh).

c. To ensure that cool electricity is supplied that satisfies the required cool demand loads for each period, this restriction must be observed:

$$P^t_{ce} + H^t_{ca} = L^t_{cool.} \quad (20)$$

Where $L^t_{cool.}$ it is cool power demand load in (KWh).

4. Objuctive function model

In order to obtain the minimal cost function CF in ($), this study changed its multi-objective goal to a single aim by considering emission cost as a monetary notion. The electricity price is considered as time-varying, reflecting time-of-use tariffs over the scheduling horizon.

$$CF = \min \sum_{t=1}^{24} [\, C^t_{MT} + {SUC_{MT}}^t + {SDC_{MT}}^t + C^t_{om.MT} + {C_{FC}}^t + {SUC_{FC}}^t + {SDC_{FC}}^t + C^t_{om.FC} + {C_{\text{DG}}}^t + {SUC_{DG}}^t + SDU^t_{DG} + C^t_{om.DG} + {C_{GB}}^t + C^t_{om.GB} + C^t_b + C^t_{hs} + C^t_{e.UG} + C^t_{h.UG} + C^t_{Emi.}] \quad (21)$$

5. The suggested CCHP system

Figure 2 depicts the suggested smart CCHP system's schematic layout. The CCHP provides loads for power, heating, and cooling. An electric grid, a heating system, and a cooling system make up the CCHP system. Together, these systems permit energy flow and deliver their load within an economical and environmentally sustainable frameworkThe electric system includes fuel cells (FCs), diesel generators (DEs), microturbine-based CHPs, wind turbines (WTs), solar panels (PVs), and storage batteries (SBs) as well as other distributed generators (DGs). In order to recover waste heat from the CHP generator, the heating system consists of a gas boiler (GB), electric heater (EH), heat storage tank (HS), and heat recovery (HR). An absorption chiller (AC) and an electric chiller (EC) make up the cooling system. Whereas FC and GB use NG to create both thermal and electric energy, the CHP uses natural gas as fuel to produce both at the same time. The EH also generates heat from electricity.

ble 1 lists the hourly needs for thermal and electrical energy as well as the associated energy Also shows the generating profiles of wind turbine (WT) and photovoltaic (PV) systems. These facts come from reliable research. 300 kWh and 90 kWh are the SB's rated maximum and low levels of charge, respectively, and its rated delivering and absorbing power is 90 kWh. The HS has a rated maximum stored energy of 300 kWh and a minimum stored energy of 90 kWh. The electric heater has a 350 kWh rate and GB has a 200 kWh rate. 100 kW, 30 kW, 70 kW, 120 kW, and 160 kW are the ramp rates for the CHP, FC, DE, GB, and AC, respectively. To effectively balance supply and demand, the system integrates a number of energy generating and storage technologiesThere is a minimum output power of 20, 10, 20, 5, 5, and 10 kilowatts for CHP, FC, DG, GB, and grid exchange capabilities, and a maximum output power of 300, 100, 200, 350, and 200 kW, respectively.

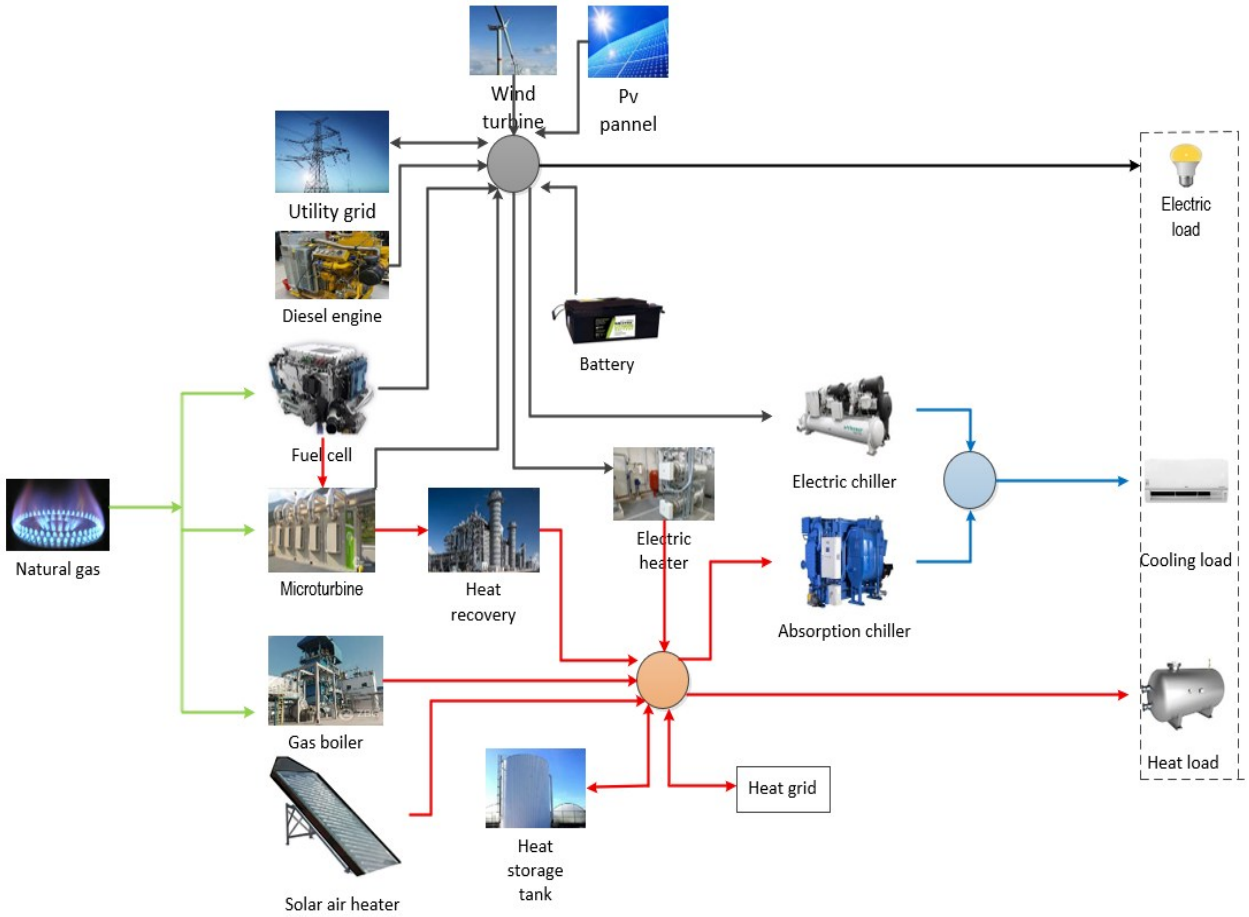

Figure 2. Schematic diagram of CCHP microgrid

Table 1. Hourly loads, prices, and renewable generation

Time (h)	$L^t_{elctr.}$ (KWh)	$L^t_{heat.}$ (KWh)	$L^t_{heat.}$ (KWh)	$\omega^t_{elect.}$ $(\$/KWh)$	$\omega^t_{heat.}$ $(\$/KWh)$	P^t_{WT} (KW)	S^t KW/m^2
t1	192	466.88	87.3	0.01	0.162	55	0
t2	177.6	481.82	61.11	0.018	0.1332	61	0
t3	132	489.29	43.65	0.02	0.1368	65	0
t4	122.4	481.82	26.19	0.018	0.1476	58	0
t5	117.6	489.29	34.92	0.025	0.1008	58	0
t6	110.4	451.94	59.36	0.045	0.054	24	100
t7	162	443.22	78.57	0.1	0.0432	40	210
t8	213.6	428.28	104.8	0.28	0.0972	34	612
t9	258	382.22	96.03	0.45	0.1152	40	665
t10	220.8	343.62	78.57	0.519	0.144	46	788
t11	295.2	336.15	89.57	0.4	0.1116	30	930
t12	368.4	290.09	113.5	0.25	0.09	31	988
t13	442.8	252.74	148.4	0.48	0.054	25	873
t14	421.2	217.88	131	0.3	0.054	25	727
t15	406.8	244.02	109.1	0.25	0.0792	36	630
t16	368.4	282.662	97.77	0.1	0.126	30	325
t17	327.6	367.28	92.56	0.035	0.1476	46	25
t18	339.6	428.28	131	0.045	0.1152	36	0
t19	361.2	520.41	150.2	0.08	0.1008	52	0
t20	420	573.95	157.14	0.12	0.0972	46	0
t21	405.6	559.01	131	0.025	0.1584	52	0
t22	421.2	555.27	104.8	0.015	0.1476	46	0
t23	375.6	539.09	101.3	0.012	0.108	46	0
t24	370.8	520.41	91.7	0.01	0.288	52	0

The coupling between electrical, heating, and cooling subsystems is achieved through the interaction of generation units and conversion devices. In particular, electricity is used to drive electric chillers, while thermal energy is utilized in absorption chillers, linking the three subsystems within the overall energy management framework. les 2–4 summarize the key system parameters, including technical characteristics, efficiency values, cost coefficients, and emission factors. These parameters are adopted as input data for the optimization framework**.**

Table 2 Energy and Heat Storage System parameter

Type	P_{ch}^{max} (KW)	P_{ch}^{min} (KW)	P_{dis}^{max} (KW)	P_{dis}^{min} (KW)	P^{max} (KW)	P^{min} (KW)	η_{ch}	η_{dis}	ω ($/KWh$)
ESS	90	1	90	1	300	90	0.9	0.9	0.06
HSS	90	1	90	1	300	90	0.9	0.9	0.0031

Table 3 Emission parameters

Source	E_{CO2} (Kg/KWh)	E_{NOx} (Kg/KWh)	E_{SO2} (Kg/KWh)	E_{PM} (Kg/KWh)
DG	0.848	0.0013	0.00125	0.00036
FC	0.489	0.00001	0.000003	0.000001
MT	0.725	0.0002	0.000004	0.000041
C_j ($/Kg$)	0.02	5	6	25

Table 4. Conventional power, heat energy and cool sources work by fuel burn parameters

Elect.	P_i^{min} KW	P_i^{max} KW	η_i	$K_{om.i}$ $/KWh	Sci ($)	Sdi ($)	UR_i (KW)	DR_i (KW)	a $/KW^2h	b $/KWh	c ($/h)
DG	20	140	-	0.01258	0.25	0.25	70	70	0.002	0.05	0.6
MT	20	200	0.3	0.026	0.1	0.1	100	100	-	-	-
FC	10	60	0.6	0.026	0.2	0.1	30	30	-	-	-
HEAT	H_i^{min} (KW)	H_i^{max} (KW)	η_i	$K_{om.i}$ $/KWh	Sci ($)	Sdi ($)	UR_i (KW)	DR_i (KW)	a ($/KW^2h$)	b ($/KWh)	c ($/h)
GB	5	100	0.73	0.0027	-	-	120	120	-	-	-
EH	0	150	0.8	0.002	-	-	-	-	-	-	-
Cce	0	100	0.85	4	-	-	150	150	-	-	-
Cca	0	200	0.85	0.8	-	-	160	160	-	-	-

For clarity, the model variables are classified into three categories: (i) decision variables, which include generation outputs and energy exchanges; (ii) parameters, such as load profiles, renewable inputs, and cost coefficients; and (iii) state variables, representing the system state over time, including stored energy levels.

6. Results and Discussion

The recommended grid has been solved by expressing it as MIQP on the UC approach in JULIA in order to get the lowest optimization cost. Using the SAH model f, the output heat power was measured experimentally in Baghdad in January, as seen in figure 1, tow scenario have been taken in this study , scenario 1 represents cchp connected with utility grid and scenario 2 with out utility grid It was found that the cost was reduced by around $739 when CCHP was connected to the main grid.

Figure 3 shows electrical power generation in scenario 1 , that the MT is running most time serve heat and power needs for the most schedule period. Furthermore, the FC runs around the clock to serve the electric demands, using max power during hours from 10am to 3pm at load is high. Also FC operate at max limit from 10 am to 4 pm with renewable resources, the time becomes for electric marketing.

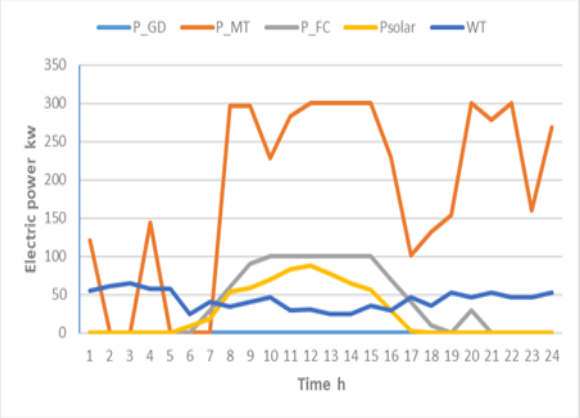

Figure 3 *Optimal Electrical power Schedule with electrical Load scenario 1*

Figure 4 illustrates FC is operating at maximum capacity due to increased demand, in addition to the MT running continuously, which increases costs in scenario 2 compared to brevious. While the diesel engine is still shut down at lower power to achieve the lowest system cost, due to the high fuel cost and high maintenance, therefore this achieves the required objective function in the proposed system at the lowest cost and with the lowest emissions.

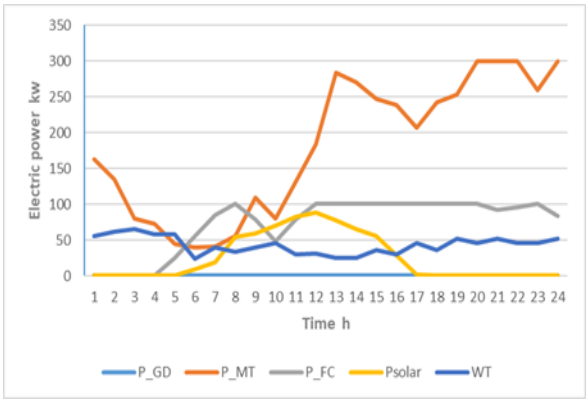

Figure 4 Optimal Electrical power Schedule with electrical Load scenario 2

The heating system's optimal hourly planning in the tow scenario is shown in Figures 5 and 6, in scenario 2, it is seen that MT supplies heat throughout the day to offer additional heat energy sources for the heat load throughout the day in order to satisfy the increased demand brought on by the exchange limitation. Furthermore, in contrast to scenario 1 in Figure 5 the GB is run continuously at maximum capacity. Compared to the GB, the EH is dedicated to less hours. This is because the electric system determines the EH's heat energy, where demand for electricity is high and the electric energy price is higher during the EH's uncommitted hours.

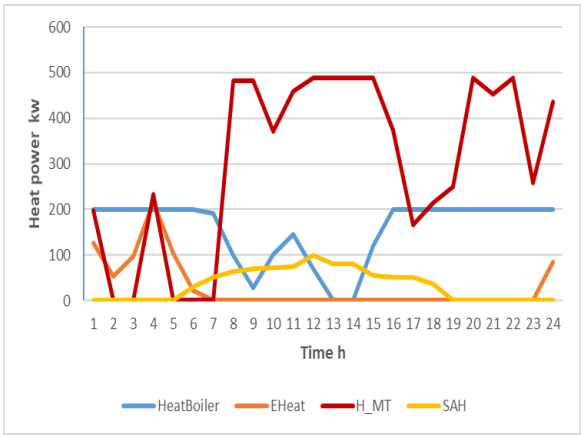

Figure 5 Optimal Heat power Schedule with heat Load scenario 1

In Senrio 2, the EH is not turn on all day due to its high electricity cost, The solar heater contributes heat during solar power availability, especially at peak times around 1 pm, and the system depended on it because it is free. As shown in figure 6.

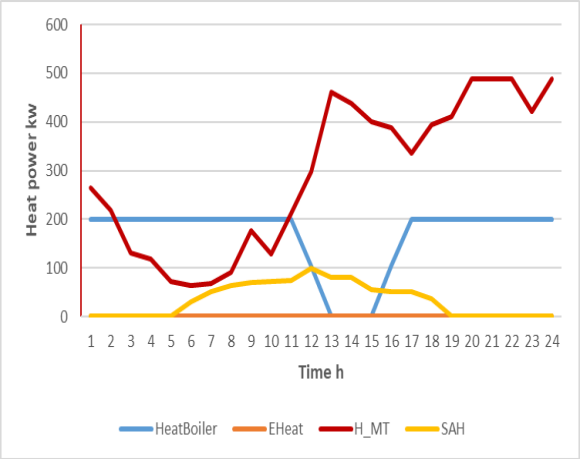

Figure 6. Optimal Heat power Schedule with heat Load scenario 2

Figure 7 illustrates the battery charged in four times as a result of the availability of power and discharged during periods of high price in order to save energy and make profit.

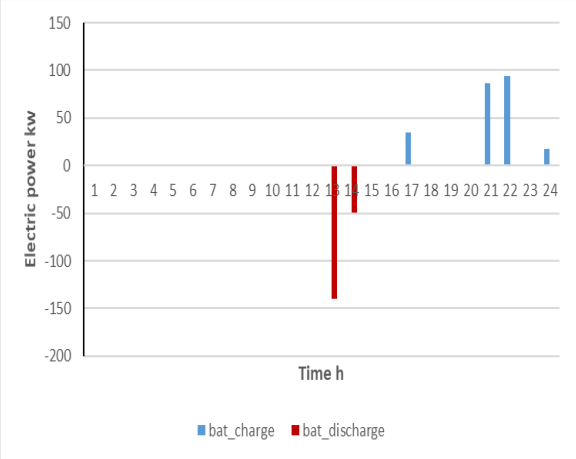

Figure 7. power Schedule of BAT in scenario 1

Figure 8, however, it was only charged at the end of the day due to a lack of power caused by the power cut in scenario 2.

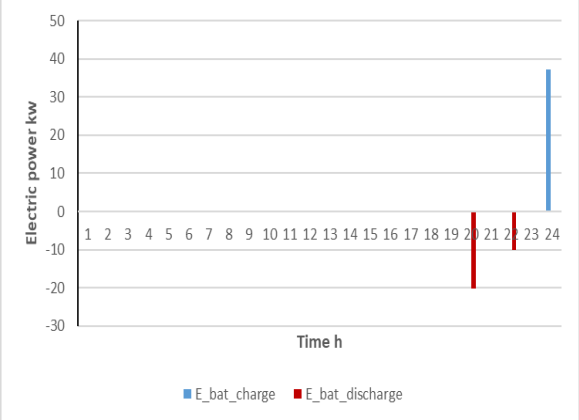

Figure 8. power Schedule of BAT in scenario 2

Figure 9 demonstrates that in scenario 1, the CCHP system exports the most electricity to the grid system between 8 a.m. and 15 p.m. since prices are at their highest and the electric demand is at its lowest when there is enough solar and wind energy. This is to reduce the CCHP system's costs and boost its income.

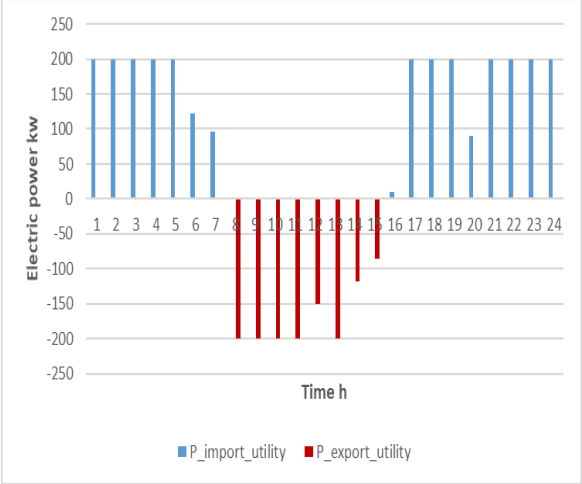

Figure 9. Optimal electric power exchange with utility in scenario 1

Figure 10 shows the heat exchange with utility in scenario 1 that refers to export from 7 am to 16 pm because the price is high to make sure profit while the other periods import despite the low price due to the load is high.

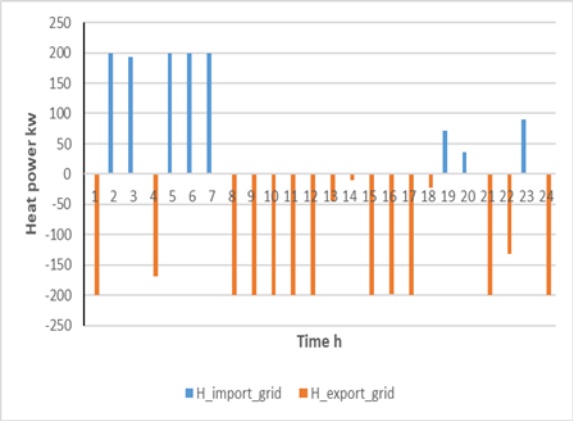

Figure10. optimal heat exchange with utility grid in scenario 1

The cool power in scenario 1 represents in Figure 11 notce that AC chiller uncommitted until hour 11 to 16 because need energy and this time the load is low and heat generation is high, but EC chiller operates anthor time because the electric load is low and the renewable energy sourse is abundand.

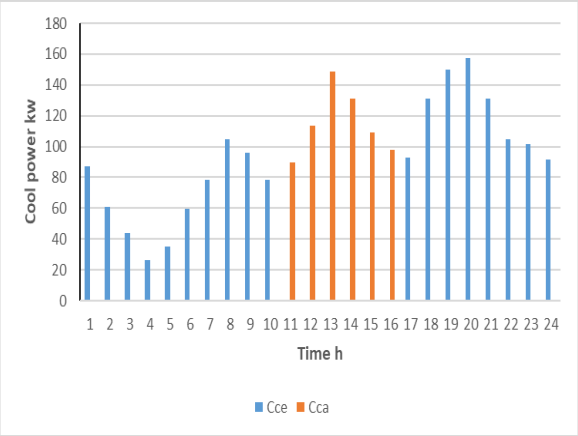

Figure 11. Cool power Schedule in scenario 1

Figure 12 explains cool power from electric chiller whole the day in scenario 2 the system then resorts to covering the electrical load, and therefore there is no excess heat to operate AC.

Compared with existing studies, the proposed model shows enhanced performance in terms of both economic and environmental aspects. Specifically, the system achieves a noticeable reduction in operational cost and emissions due to the efficient integration of renewable energy sources and improved scheduling strategy. These results indicate the effectiveness of the proposed optimization framework over conventional approaches reported in the literature.

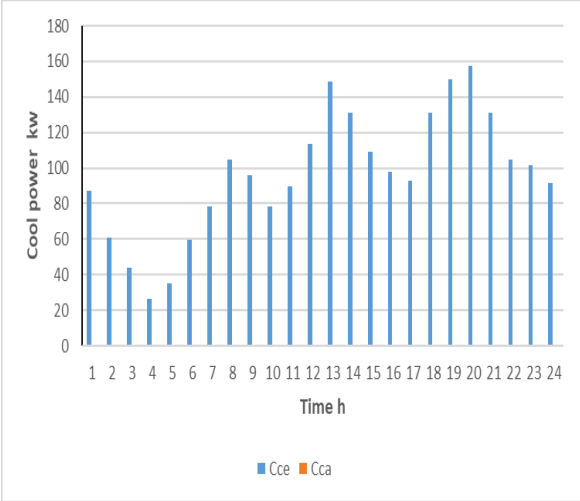

Figure 12. Cool power Schedule in scenario 2

6. Conclution

The goal of this article is to reduce the overall cost of operating a CCHP system. The system is formulated UCMIQP, which involves energy exchange between heating, cooling, and electric systems. The interaction between systems is taken into account by the UC. This research covers two scenarios: one in which the CCHP has connections to the utility grid, and the other in which it is disconnected. The results of the Julia program show the superior performance in scenario 1 in terms of minimal operating cost, which is based on the system's optimum functioning because of UC strategy.

The simulation findings demonstrate that transporting energy across many systems and changing its form reduces total operating and emission costs, while SB and HS are controlled to minimize the overall cost for both scenarios. The proposed approach can be implemented in practical microgrid systems, particularly in residential and industrial sectors, to enhance energy efficiency, reduce operational costs, and support sustainable energy management. Future work will consider uncertainty modeling of renewable energy sources to further improve the robustness of the optimization framework.

Funding

None.

Conflicts of Interest

The authors declare no conflict of interest, if it was available.

Nomenclature

UR_i	Ramp up power (KW)
DR_i	Ramp down power (KW)
$K_{om.}$	maintenance cost rate coefficient ($\$/KWh$)
η	Efficiency (%)
H	Heat Power (KW)
P	Product power (KWh)
P_G	Power generated by diesel generator (kW)
P_M	Power generated by microturbine (kW)
P_F	Power generated by fuel cell (kW)
E_load	Electrical load demand (kW)
H_load	Thermal load demand (kW)
C_load	Cooling load demand (kW)
C	Cost ($)
ω	Price ($\$/KWh$) or ($\$/m^2$)
U	On/ off state (1 or 0)
$C_{om.}$	Maintenance cost ($)
Bat	Battery
a	cost coefficient in ($\$/KW^2h$)
b	cost coefficient in ($\$/KWh$)
c	cost coefficient in ($\$/h$)
S^t	Solar radiation in (KW/m^2)
t	Time period (h)
$SOC_{}^{t}$	State of Charge in (KWh)
ch	Charging in (KWh)
dic	Discharging (KWh)
MT	Microturbine
HR	Heat Recovery
WT	Wind Turbine
PV	Photo voltage Panel
SAH	Air Solar Heater
Cce	Cool of Electric chiller
Cca	Cool of absorber chiller
EH	Electrical Heater
ESS	Energy Storage System
HSS	Heat Storage System
CCHP	Compound Cool ,Heat and Power
UC	Unit commitment

References

[1] D. Anastaselos, E. Giama, and A. M. Papadopoulos, "An assessment tool for the energy, economic and environmental evaluation of thermal insulation solutions," Energy and Buildings, vol. 41, no. 11, pp. 1165–1171, Nov. 2009, doi: 10.1016/j.enbuild.2009.06.003.

[2] W. Stanek, W. Gazda, and W. Kostowski, "Thermo-ecological assessment of CCHP (combined cold-heat-and-power) plant supported with renewable energy," Energy, vol. 92, pp. 279–289, Dec. 2015, doi: 10.1016/j.energy.2015.02.005.

[3] E. Assareh et al., "Techno-economic analysis of combined cooling, heating, and power (CCHP) system integrated with multiple renewable energy sources and energy storage units," Energy and Buildings, vol. 278, Jan. 2023, doi: 10.1016/j.enbuild.2022.112618.

[4] Y. Kuang, M. Hu, R. Dai, and D. Yang, "A Collaborative Decision Model for Electric Vehicle to Building Integration," Energy Procedia, vol. 105, pp. 2077–2082, 2017, doi: 10.1016/j.egypro.2017.03.586.

[5] Q. Wang, Y. Xiao, H. Tan, and M. A. Mohamed, "Day-Ahead scheduling of rural integrated energy systems based on distributionally robust optimization theory," Applied Thermal Engineering, 2024.

[6] F. Li, J. Su, and B. Sun, "An optimal scheduling method for an integrated energy system based on an improved k-means clustering algorithm," Energies, 2023.

[7] D. Maraver, A. Sin, J. Royo, and F. Sebastián, "Assessment of CCHP systems based on biomass combustion for small-scale applications through a review of the technology and analysis of energy efficiency," Applied Energy, 2013.

[8] J. Wang, S. You, Y. Zong, C. Træholt, Y. Zhou, and S. Mu, "Optimal dispatch of combined heat and power plant in integrated energy system: A state-of-the-art review and case study of Copenhagen," Energy Procedia, vol. 158, pp. 2794–2799, 2019, doi: 10.1016/j.egypro.2019.02.040.

[9] V. Tiwari, H. M. Dubey, M. Pandit, and S. R. Salkuti, "CHP-based economic emission dispatch of microgrid using Harris Hawks optimization," Fluids, vol. 7, no. 7, Jul. 2022, doi: 10.3390/fluids7070248.

[10] H. Ahn, W. Miller, P. Sheaffer, V. Tutterow, and V. Rapp, "Opportunities for installed combined heat and power (CHP) to increase grid flexibility in the US," Energy Policy, vol.

157, Oct. 2021, doi: 10.1016/j.enpol.2021.112485.

[11] W. Gu, Z. Wu, and X. Yuan, "Microgrid economic optimal operation of the combined heat and power system with renewable energy," IEEE PES General Meeting, 2010, doi: 10.1109/PES.2010.5590140.

[12] Z. Ma et al., "Peer-to-peer trading solution for microgrids in Kenya," IEEE PES/IAS PowerAfrica, pp. 420–425, 2018, doi: 10.1109/POWERAFRICA.2018.8520980.

[13] A. Parisio, E. Rikos, and L. Glielmo, "Stochastic model predictive control for economic/environmental operation management of microgrids: An experimental case study," Journal of Process Control, vol. 43, pp. 24–37, Jul. 2016, doi: 10.1016/j.jprocont.2016.04.008.

[14] G. F. Smaisim, A. M. Abed, S. K. Hadrawi, H. S. Majdi, and A. Shamel, "Modelling and optimization of combined heat and power system in microgrid based on renewable energy," Clean Energy, vol. 7, no. 4, pp. 735–746, Aug. 2023, doi: 10.1093/ce/zkad012.

[15] P. Hu, C. Cao, and S. Dai, "Optimal dispatch of combined heat and power units based on particle swarm optimization with genetic algorithm," AIP Advances, vol. 10, no. 4, Apr. 2020, doi: 10.1063/1.5145074.

[16] R. Yuan, J. Ye, J. Lei, and T. Li, "Integrated combined heat and power system dispatch considering electrical and thermal energy storage," Energies, vol. 9, no. 6, Jun. 2016, doi: 10.3390/en9060474.

[17] O. Erixno, N. A. Rahim, F. Ramadhani, and N. N. Adzman, "Energy management of renewable energy-based combined heat and power systems: A review," Sustainable Energy Technologies and Assessments, vol. 51, Jun. 2022, doi: 10.1016/j.seta.2021.101944.

[18] C. A. Salman, H. Li, P. Li, and J. Yan, "Improve the flexibility provided by combined heat and power plants (CHPs) – a review of potential technologies," Process Integration and Optimization for Sustainability, vol. 1, Jan. 2021, doi: 10.1016/j.prime.2021.100023.

[19] [19] C. Dobre, M. Costin, and M. Constantin, "A review of available solutions for implementation of small–medium combined heat and power (CHP) systems," Inventions, vol. 9, no. 4, Aug. 2024, doi: 10.3390/inventions9040082.

[20] [20] E. Jafari, S. Soleymani, B. Mozafari, and T. Amraee, "Optimal operation of a micro-grid containing energy resources and demand response program," International Journal of Environmental Science and Technology, vol. 15, no. 10, pp. 2169–2182, Oct. 2018, doi: 10.1007/s13762-017-1525-6.

[21] D. Ma, L. Zhang, and B. Sun, "An interval scheduling method for the CCHP system containing renewable energy sources based on model predictive control," Energy, vol. 236, Dec. 2021, doi: 10.1016/j.energy.2021.121418.

[22] J. Jia, H. Chen, H. Liu, T. Ai, and H. Li, "Thermodynamic performance analyses for CCHP system coupled with organic Rankine cycle and solar thermal utilization under a novel operation strategy," Energy Conversion and Management, vol. 239, Jul. 2021, doi: 10.1016/j.enconman.2021.114212.

[23] S. Soheyli, M. H. Shafiei Mayam, and M. Mehrjoo, "Modeling a novel CCHP system including solar and wind renewable energy resources and sizing by a CC-MOPSO algorithm," Applied Energy, vol. 184, pp. 375–395, Dec. 2016, doi: 10.1016/j.apenergy.2016.09.110.

[24] F. Ren, Z. Wei, and X. Zhai, "Multi-objective optimization and evaluation of hybrid CCHP systems for different building types," Energy, vol. 215, Jan. 2021, doi: 10.1016/j.energy.2020.119096.

[25] Y. Ge, J. Han, Q. Ma, and J. Feng, "Optimal configuration and operation analysis of solar-assisted natural gas distributed energy system with energy storage," Energy, vol. 246, May 2022, doi: 10.1016/j.energy.2022.123429.

[26] C. He, Q. Zhang, J. Ren, and Z. Li, "Combined cooling heating and power systems: Sustainability assessment under uncertainties," Energy, vol. 139, pp. 755–766, Nov. 2017, doi: 10.1016/j.energy.2017.08.007.

[27] Y. Ruan, Z. Liang, F. Qian, H. Meng, and Y. Gao, "Operation strategy optimization of combined cooling, heating, and power systems with energy storage and renewable energy based on deep reinforcement learning," Journal of Building Engineering, vol. 65, Apr. 2023, doi: 10.1016/j.jobe.2022.105682.

[28] A. Song, J. Zhu, P. Zhang, N. Chang, and Z. Cui, "Experimental research on solar and geothermal energy coupling power generation system," Energy Procedia, vol. 158, pp. 5982–5987, 2019, doi: 10.1016/j.egypro.2019.01.522.

[29] Y. Li et al., "Optimal stochastic operation of integrated low-carbon electric power, natural gas, and heat delivery system," IEEE Transactions on Sustainable Energy, 2017. Available: https://ieeexplore.ieee.org/abstract/document/7982799/

[30] D. Xie, Y. Lu, J. Sun, C. Gu, and J. Yu, "Optimal operation of network-connected combined heat and powers for customer profit maximization," Energies, 2016. Available: https://www.mdpi.com/1996-1073/9/6/442

[31] H. Farzin, M. Fotuhi-Firuzabad, and M. Moeini-Aghtaie,"Stochastic energy management of microgrids during unscheduled islanding period,"IEEE Transactions on Industrial Electronics, vol. 63, no. 11, pp. 7039–7048, Nov. 2016, doi: 10.1109/TIE.2016.2590380.

[32] N. P. Bayendang, M. T. Kahn, and V. Balyan, "Combined cold, heat and power (CCHP) systems and fuel cells for CCHP applications: A topological review," Clean Energy, vol. 7, no. 2, pp. 436–491, 2023, doi: 10.1093/ce/zkac079.

[33] Y. Li, Y. Zou, Y. Tan, Y. Cao, X. Liu, M. Shahidehpour, S. Tian, and F. Bu, "Optimal stochastic operation of integrated low-carbon electric power, natural gas, and heat delivery system," IEEE Transactions on Sustainable Energy, vol. 9, no. 1, pp. 273–283, Jan. 2018. doi: 10.1109/TSTE.2017.2728098.

[34] D. Zhang et al.,"Carbon emission reduction analysis of CHP system driven by biogas based on emission factors," Energy and Built Environment, vol. 4, no. 5, pp. 576–588, 2023, doi: 10.1016/j.enbenv.2022.05.002.

[35] M. S. A. Ghafoor, M. K. Al-Saadi, and A. A. Jaddoa, "Comparative Study on the Performance of a Solar Air Heater Using Aluminum Soda Cans with 'Different Arrangements'," Frontiers in Heat and Mass Transfer, vol. 23, no. 1, 2025. doi: 10.32604/fhmt.2025.064025.

[36] Y. Zhong, D. Xie, S. Zhai, and Y. Sun, "Day-Ahead Hierarchical Steady State Optimal Operation for Integrated Energy System Based on Energy Hub," Energies, vol. 11, no. 10, p. 2765, Oct. 2018. doi: 10.3390/en11102765.